Arabian Journal for Science and Engineering (2019) 44:3883–3904
https://doi.org/10.1007/s13369-018-03712-7

RESEARCH ARTICLE - COMPUTER ENGINEERING AND COMPUTER SCIENCE

# Improved Many-Objective Optimization Algorithms for the 3D Indoor Deployment Problem

Sami Mnasri[1] · Nejah Nasri[2] · Adrien van den Bossche[1] · Thierry Val[1]

Received: 31 March 2017 / Accepted: 31 December 2018 / Published online: 12 January 2019


**Abstract**
Compared with the two-dimensional deployment, the three-dimensional deployment of sensor networks is more challenging. We studied the problem of 3D repositioning of sensor nodes in wireless sensor networks. We aim essentially to add a set of nodes to the initial architecture. The positions of the added nodes are determined by the proposed algorithms while optimizing a set of objectives. In this paper, we suggest two main contributions. The first one is an analysis contribution where the modelling of the problem is given and a set of modifications is incorporated on the tested multi-objective evolutionary algorithms to resolve the issues encountered when resolving many-objective problems. These modifications concern essentially an adaptive mutation and recombination operators with neighbourhood mating restrictions, the use of a multiple scalarizing functions concept and the incorporation of the reduction in dimensionality. The second contribution is an application one, where an experimental study on real testbeds is detailed to test the behaviour of the enhanced algorithms on a real-world context. Experimental tests followed by numerical results prove the efficiency of the proposed modifications against original algorithms.

**Keywords** 3D indoor deployment · Experimental validation · Many-objective optimization · Neighbourhood · Adaptive operators

## 1 Introduction

In wireless sensor networks (WSNs), the 3D deployment is a strategy that defines the number of nodes, their positions and the network topology in a 3D space. In fact, the process of deploying and positioning nodes greatly influences the efficiency of the network. On both 2D and 3D spaces, the coverage is the most considered objective when deploying nodes in WSNs. It can be considered as a measurement of the reliability and the network quality of service. A full probability of coverage cannot be ensured by increasing the number of sensors when deploying nodes randomly. Furthermore, it is expensive to maintain high-density networks on a large scale. Hence, other approaches should be proposed to resolve these issues and to enhance the coverage degree of the initial deployment. In the literature, different coverage problems are investigated [1]. Among them are area coverage, target coverage, barrier coverage, sweep coverage and $k$-coverage problem.

In most 3D deployment formulations, the coverage problem is proven and considered as a NP-hard problem [2]. Hence, this problem is unsolved using deterministic approaches like the Branch and Bound especially for large-scale instances. Therefore, in this study, the problem is defined formally and a heuristic approach based on modified algorithms is proposed to resolve it. Specially, we are interested in deploying WSN in smart buildings areas. The model we suggest differs from existing models thanks to the fact that

**Electronic supplementary material** The online version of this article (https://doi.org/10.1007/s13369-018-03712-7) contains supplementary material, which is available to authorized users.

✉ Sami Mnasri
Sami.Mnasri@fsgf.rnu.tn

Nejah Nasri
nejah.nasri@isecs.rnu.tn

Adrien van den Bossche
vandenbo@irit.fr

Thierry Val
val@irit.fr

[1] UT2J, CNRS-IRIT (RMESS), University of Toulouse, Bureau C107, Batiment C, 1 Place Georges Brassens, 31700 Blagnac, Toulouse, France

[2] ENIS, LETI, University of Sfax, Sfax, Tunisia

it integrates a realistic coverage model based on experimental assumptions, and a hybrid localization approach in one model. For more details about the 3D deployment problem, we can refer to the surveys in [3,4].

The essential goal in this study is minimizing the number of deployed nodes and maximizing the coverage and localization rates. Other objectives which are linked to the coverage and localization issues are also considered, such as minimizing the energy consumption and maximizing the network lifetime. Achieving these objectives together makes the problem more complex and harder to resolve using classical optimization algorithms, hence the need to improve these optimization algorithms.

Indeed, the community of evolutionary multi-objective optimization (EMO) is increasingly interested in many-objective optimization (MaOO) aiming at simultaneously optimizing more than three objectives. This is essentially because of the unlike behaviours of EMO algorithms in MaOO against optimization with three objectives or less. In this regard, several EMO algorithms, known for a high performance when resolving two and three objective problems, encounter difficulties with problems having spaces with high-dimensional objectives. Thus, a big challenge for both practitioners and researchers in the area is faced. Different studies are proposed in order to resolve many-objective optimization problems (MaOP). However, existing approaches are limited to a small number of studies on a few number of test problems. The major difficulties encountered by multi-objective evolutionary algorithms (MOEAs) when resolving MaOPs can be summarized as follows:

- Inefficiency of the Pareto-based EMOs.
- Inaccuracy of the density estimation.
- Ineffectiveness of the recombination operation.
- Exponential increase in cost (time and space).
- Difficulty in representing the trade-off surface.

The rest of the paper is structured as follows: A set of related recent works are investigated in Sect. 2 Then, the problem formulation is detailed in Sect. 3, and a set of well-justified modifications incorporated into the optimization algorithms are presented in Sect. 4. Afterwards, an experimental study based on real testbeds is discussed in Sect. 5. Next, the behaviour of the tested modified algorithms is assessed using the hypervolume (HV) metric in Sect. 6. Finally, Sect. 7 concludes the paper.

## 2 Related Works

In the literature, different works aim at resolving the problem of deploying sensors in wireless networks. Table 1 illustrates a comparison between the recent approaches used to resolve the deployment problem in WSN.

More details on the coverage problems and their resolving methods can be found on the following recent surveys: [20–22].

Nevertheless, other than the 3D deployment, different other methods aim to ensure the optimal coverage in wireless networks. Table 2 illustrates a comparison between our approach and another one called 'the collision free data link layer'.

Among the main drawbacks of these studies is the non-consideration of the many-objective case of the problem. Even more, the majority of these studies did not test the proposed approaches on real-world problems which are more complex. Hence, the proposed contributions can be summed up as follows: First, we suggest a set of well-studied modifications applied to the $\in$-NSGA-II [24], the U-NSGA-III [25] and the MOEA/DD [26] algorithms. Except the NSGA-II, these modifications are applied for the first time on the proposed algorithms. These modifications concern an adaptive neighbourhood-based variation of the operators and a multiple use of scalarizing functions. Moreover, in most studies, the performance of the algorithm is not proven by empirical real-world scenarios and only simulations or theoretical multi-objective problems (like ZDT or DTLZ) are used. Thus, another major contribution is that in this study, experimental tests are given based on a real-world environment allowing demonstrating the real contribution of the modification through the proposed algorithms. Thus, the originality of this work compared to other works appears in the used algorithms relying on real measurements allowing them to provide more realistic hypothesis.

## 3 The Problem Formulation

### 3.1 Network Architecture

The following types of nodes are considered:

- *Fixed nodes* stationary nodes representing the nodes initially installed in the RoI (region of interest) with known positions. They may be distributed randomly, or according to a strategy. In our simulations, they are disseminated according to the distribution law of the simulator. In our experiments, they are disseminated according to the applicative needs of the users.
- *Mobile nodes* targets representing the persons to control which are equipped with a sensor receiving and transmitting the signal. Its positions are predefined but susceptible to be changed. In simulations, the mobile node is used as a launcher of the first message, while in experiments, this type of nodes is attached to a moving person in the RoI in order to take measures in different positions.

**Table 1** Comparison between different recent works resolving the deployment problem in WSNs

| References | Application(s) | Space | Sensing model | Approach | Objective(s) | (+)Advantages/(−)Draw backs/(*)Characteristics |
|---|---|---|---|---|---|---|
| Jiang et al. [5] | Thermal sensor placement in smart grid | 2D | Stochastic | A genetic approach based on a gappy proper orthogonal decomposition (GPOD-GA) | Minimize the thermal sensor number | (−) A single objective is considered<br>(−) No evaluation of the proposed approach using known metrics |
| Alia and Al-Ajouri [6] | No application is given | 2D | Deterministic | Harmony search-based algorithm | Maximizing the coverage, maximizing the deployed sensor number | (−) A simple model of the network<br>(−) A bi-objective model: only two objectives are considered<br>(−) No simulator is used: only MATLAB results are presented |
| Sweidan and Havens [7] | Context of terrain-aware wireless sensor networks | 2D | Deterministic | Normalized genetic approach (NGA), artificial immune system (AIS) approach and particle swarm optimization (PSO)-based approach | Minimize the cost of mobility and maximize the coverage | (−) High execution time of the proposed AIS and NGA |
| Khalfallah et al. [8] | Water river monitoring: a 3D underwater deployment for detecting the pollution in rivers | 3D | Deterministic | '3D-UWSN-Deploy' : a 'divide and conquer' technique relying on a mixed integer linear programming and a sub-cube tessellation of the monitored field | Number of deployed sensors | * Main steps of the proposed strategy: *generating sub-cubes tessellation*, *generation sub-cubes tree* and *optimal solution of sub-cube* |
| | | | | | Connectivity | ∗The CPLEX 12.5.1.0 solver is used |
| | | | | | Quality of monitoring (QoM) | (+) Large-scale deployment : About 500 sensors are used<br>(−) No dedicated simulator is used<br>(−) No experimental study is proposed |

**Table 1** continued

| References | Application(s) | Space | Sensing model | Approach | Objective(s) | (+)Advantages/(−)Draw backs/(*)Characteristics |
|---|---|---|---|---|---|---|
| Brown et al. [9] | 3D indoor video sensor network deployment | 3D | Heuristic | A greedy heuristic algorithm based on an enhanced depth-first search | 3D indoor space coverage | (+) The proposed approach reduces the required video sensors by up to half over a baseline algorithm<br>(+) A lattice grid model for a discrete real-world applicable environment |
| Liu et al. [10] | Heterogeneous camera sensor networks | 3D | Predictive | $k$-coverage estimation problem in heterogeneous camera sensor networks with boundary deployment | $k$-coverage | (+) A detailed mathematical model is given<br>(−) Only MATLAB is used to construct the simulation scenario (no dedicated simulator is used) |
| Cotta et al. [11] | Placement of suicide bomber detectors | 2D | Heuristic | GRASP: a greedy randomized adaptive search procedure<br>HC: a hill climber<br>EA: an evolutionary algorithm<br>UMDA: a Univariate marginal distribution algorithm | Different objectives | (+) Different numbers of objectives are considered<br>* The Hill climbing technique obtains the best results<br>(−) The Hill climbing is a time-consuming algorithm |
| Wu et al. [12] | Placing the minimum set of wireless sensors at locations in a constrained 3D space | 3D | Heuristic | A genetic algorithm based approach | Number of deployed sensors<br>$k$-coverage<br>Connectivity | (−) The performance evaluation is simulation-based<br>(−) The problem is tested only for small and medium-scale cases |

**Table 1** continued

| References | Application(s) | Space | Sensing model | Approach | Objective(s) | (+)Advantages/(−)Draw backs/(*)Characteristics |
|---|---|---|---|---|---|---|
| Hu et al. [13] | Energy harvesting cooperative wireless sensor networks | – | Deterministic | A grid deployment algorithm relying on a Graphene-based Energy Cooperative Charging (GECC) strategy and a Graphene-based Opportunistic Cooperative Routing (GOCR) strategy | Energy efficiency<br>Network connectivity<br>Network lifetime | (−) The proposed approach is not compared with other known deployment approaches |
| Zhang et al. [14] | Deployment of post-disaster environments using unmanned aerial vehicle (UAV) | 3D | Stochastic | A stochastic geometrical framework estimating the coverage probability | Coverage probability | (−) The proposed geometrical framework is dedicated to the problem of post-disaster deployment and cannot be easily generalized to other deployment problems |
| Yüce et al. [15] | Hybrid Ultra-Dense Networks | – | Heuristic | An optimization framework based on genetic algorithms (GA) | Coverage | (+) A case study is detailed and discussed<br>(−) A standard version of the GA is proposed, without resolving the difficulties that GA encounter when resolving real-world many-objective problems (difficulties like the local optima and exponential increase in complexity) |
| Cao et al. [16] | Monitoring maritime environments | 3D | Heuristic | A distributed multi objective evolutionary parallel algorithm | Coverage<br>Reliability<br>Lifetime | (+) The proposed algorithm is parallel, cooperative, multi-objective and largescale<br>(+) The Wilcoxon test results and the average rankings of algorithms (Friedman) are computed and discussed<br>(−) An uncertain coverage model is used based on distance-sensing and angularsensing |

**Table 1** continued

| References | Application(s) | Space | Sensing model | Approach | Objective(s) | (+)Advantages/(−)Draw backs/(*)Characteristics |
|---|---|---|---|---|---|---|
| Cui et al. [17] | Non-uniform 3D wireless sensor network in forest environment | 3D | Heuristic | A genetic algorithm and a minimum spanning tree strategy | Convergence Connectivity | * A new fitness function, which considers the connectivity and the convergence, is proposed |
| Zhou et al. [18] | Distributed detection network in complex electromagnetic environments | 2D | Heuristic | An improved particle swarm optimization algorithm | Coverage | (+) The proposed PSO is compared with another heuristic evolutionary algorithm (SPSO) and another deployment approach (virtual force algorithm) |
| | | | | | Localization | (−) The used signal propagation model and RSSD location algorithm are simplistic |
| Hildmann et al. [19] | Deployment of indoor distributed antenna systems | 2D | Heuristic | A particle swarm optimization algorithm with intra-floor and inter-floor optimization | Coverage | (+) The scalability and the quality of solutions are evaluated |
| | | | | | Power budget | (−) The modelling of the problem is not well explained (assumptions and constraints are not detailed) |
| | | | | | Deployment cost | |

**Table 2** Comparison between the *3D deployment* and the *free collision data link layer* approaches

| | Our approach (3D indoor deployment for coverage problem) | Avoidance of collision data link layer (Meribout et al. [23]) |
|---|---|---|
| Type of deployment | Offline (nodes are added after running the last iteration of the optimization algorithm) Indoor | Online (a real-time application) Outdoor |
| Considered objectives | Different objectives are considered (from 2 to 8): coverage, connectivity, localization, etc. | Security, reliability, link collision |
| Used method for resolving the coverage problem | Evolutionary optimization | Data link free collision |
| Advantages | Real experimentation are given and discussed | Reliability and security of real-time data transfer is taken into account |
| Drawbacks | The used approach is complex: It is based on adaptive operators, neighbourhood mating, multiple scalarizing functions and dimensionality reduction | Real deployment is high cost (more than simulations) since it requires a base station every 125 m of the road |

– *Nomad nodes* to be added in order to improve the 3D deployment. Its positions are defined by the tested algorithms.

## 3.2 Notation

- Sets

$S^{\text{ps}}$ represents the different sites where to install nodes.
$S^{\text{tn}}$ represents the different types of nodes.
$S^{\text{mt}}$ represents the set of mobile targets to detect.
$S^{\text{nd}}$ represents the set of nodes. Each one has a type in $S^{\text{tn}}$ and is deployed in site in $S^{ps}$.

- Parameters

*Nmt* the number of targets.
*Nsa* the number of deployed stationary anchors.
*Nnd* the number of nomad nodes to add.
*Dg* the degree of coverage of a target, which is the minimum needed number of nodes to localize it.
$L > 0$ the total lifetime of the network, $L_i$ is the lifetime of the sensor $i \in S^{\text{nd}}$.
$Hw_b^a$ the hardware cost for deploying a node having a type $a \in S^{\text{tn}}$, to be installed at a site $b \in S^{\text{ps}}$.
$Coord$ the 3D position of a sensor: its coordinates $(i, j, k)$ in the indoor space.
$PowT_i^r$ the emitted RSSI ((received signal strength indicator) is the transmitted power of the signal) of the sender node $i \in S^{\text{nd}}$.
$PowR_i^r$ the emitted RSSI (the received power of the signal) at a distance r from the sender node $i \in S^{\text{nd}}$.
$Pow_{\min}^a$ a threshold representing the minimum needed RSSI transmitted by (received from) a node having a type $a \in S^{\text{nd}}$ to detect it.

- Decision variables

*CvPos* a 0–1 variable, equal to 1 if there is a node covering the position with the minimum needed power of transmission.
$Rt_{qq'}^{bc}$ a 0–1 variable, equal to 1 if the link $(q, q')$ to route the traffic flow from a source $b \in S^{\text{ps}}$ to a destination $c \in S^{\text{ps}}$ is the shortest.
$A_{tb}$ a 0–1 variable, equal to 1 if a node in the site $b \in S^{\text{ps}}$, can receive a signal from a target in a position $t \in S^{\text{mt}}$.
$Rcv_{aa'}$ a 0–1 variable, equal to 1 if a node at a site $a \in S^{\text{ps}}$ can receive a signal from a node in a site $a' \in S^{\text{ps}}$.
$Trs_{aa'}$ a 0–1 variable, equal to 1 if the node at a site $a \in S^{\text{ps}}$ can transmit a signal from a node at a site $a' \in S^{\text{ps}}$.
$Fx_b^a$ a 0–1 variable, equal to 1 if a fixed node with a type $a \in S^{\text{tn}}$ is set at a site $b \in S^{\text{ps}}$; 0 otherwise.
$Nd_b^a$ a 0–1 variable, equal to 1 if a nomad sensor with a type $a \in S^{\text{tn}}$ is set at a site $b \in S^{\text{ps}}$; 0 otherwise.

## 3.3 Objectives

- Number of nomad nodes to be added

Minimizing the number of nomad nodes to add:

$$\text{Minimize} \sum_{b \in S^{\text{ps}}} Nd_b^a \tag{1}$$

$$\text{Subject to} \sum_{b \in S^{\text{ps}}} Nd_b^a \leq Nnd \quad \forall b \in S^{\text{ps}}, a \in S^{\text{tn}} \tag{2}$$

- Deployment cost

The cost of deployment of a node ($a \in S^{\text{tn}}$) is related to its site ($b \in S^{\text{ps}}$). For example, attaching a node to a wall is considered as 'cheaper' than attaching it in the middle of the space. Then, the deployment cost is an objective to minimize,

separately, the number of nomad nodes:

$$\text{Minimize} \sum_{b\in S^{\text{ps}}} \sum_{a\in S^{\text{tn}}} Nd_b^a Hw_b^a \tag{3}$$

- Localization

To enhance the localization, at least $Dg$ anchor nodes are considered to monitor each target $t \in \text{S}^{\text{mt}}$. Then, $\sum_{s\in S^{ps}} A_{ts} \geq Dg\, \forall t \in S^{\text{mt}}$. Hence, the following function is proposed to model the localization:

$$\text{Maximize} \sum_{t\in T} \left( \sum_{b\in S^{\text{ps}}} A_{tb} - Dg \right) \tag{4}$$

$$\text{Subject to} \sum_{b\in S^{\text{ps}}} A_{tb} \geq Dg\ \forall t \in S^{\text{mt}} \tag{5}$$

- Coverage

To achieve a full coverage, at least $Dg$ nodes are used to monitor each position in the 3D indoor space. Then: $\sum_{b\in S^{\text{ps}}} CvPos \geq Dg$. Hence, the following function is proposed to model the coverage:

$$\text{Maximize} \sum_{t\in T} \left( \sum_{b\in S^{\text{ps}}} CvPos - Dg \right) \tag{6}$$

$$\text{Subject to} \sum_{b\in S^{\text{ps}}} CvPos \geq Dg \tag{7}$$

- Connectivity

Each node should have at least one incoming and one outgoing link to consider the network as connected. Thus, the connectivity probability is in general related to the strength of the received signal and the transmission range.

$$\text{Maximize}\ PowR_i^r \tag{8}$$

Subject to

$$PowR_i^r \leq Trs_{aa'} * Rcv_{aa'} * \alpha * u^{-\Phi} * PowT_i^r \tag{9}$$

where $\Phi$ is the path loss exponent and $u$ is the distance from the sender. $u = u_c \Leftrightarrow PowR_i^r = Pow_{\min}^a$ indicating that the data may be received only if the power at the receiver is higher or equal to $Pow_{\min}^a$. The transmission range $u_c$ is defined by $PowR_i^r(u = u_c) = Pow_{\min}^a$.

- Energy consumption

Because sensing and being idle energies are negligible compared to the receiving and transmitting energies, we propose a model where $E_i^{\text{elec}}$ is the dissipated energy to activate the receiver/ transmitter circuit. According to the 802.15.4 protocol used in experiments, the reception energy is generally more expensive than the transmitting one:

$$\text{Minimize} \sum E_i^{\text{transm}} + \sum E_i^{\text{recv}} \tag{10}$$

where $E_i^{\text{recv}} = E_i^{\text{elec}} * m$ and $E_i^{\text{transm}} = E_i^{\text{elec}} * m + \in_{\text{amp}} * m * d^2$ which is the energy consumed to transmit an m-bit packet to a distance d, and the energy consumed to receive the same packet is $E_i^{\text{recv}}$. $\in_{\text{amp}}$ represents the transmitter amplifier to communicate. Different constraints are considered such as constraint (11) indicating that if there is a route $Rt_{qq'}^{ab}$ passing through a sensor $a$ to another one $b$, then the sensor $a$ must be in activity:

$$Rt_{qq'}^{bc} \leq Z_a^k \tag{11}$$

where $Z_a^k$ is equal to 1 if the sensor $a$ is activated during a period k ∈ K. Besides, constraint (12) indicates that the expenditure $\text{Bt}_\text{i}$ of each sensor $i$ in energy cannot exceed the available energy in the battery of this sensor:

$$0 \leq Bt_i \leq E_0 \leq E_i^{\text{transm}} + E_i^{\text{recv}} \forall i \in S^{\text{nd}} \tag{12}$$

where $\text{E}_\text{o}$ is the initial amount of energy.

- Network lifetime

The network lifetime is often defined as the time in which the first node dissipates its energy. Several parameters affect the network lifetime such as the node density, the initial energy and the used routing strategies.

$$\text{Maximize}\ L \tag{13}$$

$$\text{Subject to}\ L = \min_{i=1,2,\ldots,\max} L_i \tag{14}$$

where max is the maximum number of nodes that may be deployed within the network. Constraint (14) indicates that the lifetime is equal to the minimum lifetime $\text{L}_\text{i}$ among all the sensors lifetimes where $L_i = Bt_i / \max(E_i^{\text{transm}} + E_i^{\text{recv}}), \forall i \in S^{\text{nd}}$.

Other constraints can be considered:

$$\sum_{q'\in S^{\text{ps}}} Rt_{qq'}^{bc} * L - \sum_{q'\in S^{\text{ps}}} Rt_{q'q}^{bc} * L = Q_c * L * Fx_b^a \forall b \in S^{\text{ps}}, a \in S^{\text{tn}} \tag{15}$$

$$\sum_{q'\in S^{\text{ps}}} Rt_{qq'}^{bc} * L + \sum_{q'\in S^{\text{ps}}} Rt_{q'q}^{\text{bc}} * L \leq Cap^{\text{nd}} * L * Fx_b^a + Cap^{\text{nd}} * L * Nd_b^a \quad \forall b \in S^{\text{ps}}, a \in S^{\text{tn}} \tag{16}$$

$$\sum_{q'\in S^{\text{ps}}} E_i^{\text{transm}} * Rt_{qq'}^{\text{bc}} * L$$

$$+ \sum_{q' \in S^{\mathrm{ps}}} E_i^{\mathrm{recv}} * Rt_{q'q}^{\mathrm{bc}} * L + Q_c * L * Fx_b^a$$

$$\leq Bt_i * Fx_b^a + Bt_i * Nd_b^a \forall a \in S^{\mathrm{ps}}, b \in S^{\mathrm{tn}} \quad (17)$$

$$\sum_{b \in S^{\mathrm{ps}}} Fx_b^a + \sum_{b \in S^{\mathrm{ps}}} Nd_b^a \leq N_{\max} + |S^{\mathrm{ps}}| - |S^{\mathrm{ps}}| * (Fx_b^a + Nd_b^a) \quad \forall a \in S^{\mathrm{ps}}, b \in S^{\mathrm{tn}} \quad (18)$$

$$0 \leq Rt_{qq'}^{\mathrm{bc}} * L \leq Wl_{bb'} * L * Fx_b^a + Wl_{bb'} * L * Nd_b^a \forall b, b' \in S^{\mathrm{ps}}, a \in S^{\mathrm{tn}} \quad (19)$$

where $Q_c$ is the rate of generating information of a sensor located at $b' \in \mathrm{S^{ps}}$, $\mathrm{Cap^{nd}}$ is the capacity (maximum amount of data a node can transmit or receive) and $\mathrm{Wl_{bb'}}$ is the wireless link (b, b′) capacity.

- Utilization of the network

To enhance the network lifetime, many nodes can be placed near to the base station. However, this may increase cost and cause a poor utilization of the resources. As a result, it is recommended to maximize the lifetime while deploying a reasonable number of nodes. Thus, the network utilization (NU) is defined as:

$$\text{Maximize } L/\sum (Fx_b^a + Nd_b^a), \quad \forall \mathrm{a} \in \mathrm{S^{ps}}, \mathrm{b} \in \mathrm{S^{tn}} \quad (20)$$

$$\text{Subject to } \sum (Fx_b^a + Nd_b^a)/L \leq (1/L^{\mathrm{up}}) \quad (21)$$

where $L^{\mathrm{up}}$ is an $L$ upper-bound.

## 4 Chromosomes Coding and Suggested Modifications in the MaOEAs

In this section, the specifications of the proposed algorithms like the manner in which chromosomes are coded are detailed. Then, a set of suggested modifications, incorporated into the many-objective algorithms, are presented. These modifications concern the use of the neighbourhood and an adaptive guided concept in mutation and recombination operators, and the use of multiple scalarizing functions in the aggregation-based approaches.

### 4.1 Chromosomes Coding for the Proposed MaOEAs

For all EMOs, the chromosome coding must be specified. Indeed, a 3D position of a node is represented by a chromosome indicating the potential locations of nomad nodes in the RoI. A point $(X, Y, Z)$ models this position. Each gene in the chromosome represents a binary digit gathering the position's value on the X, Y and Z axes. Different factors influence choosing the chromosomes population size. The most important ones are the network configuration and the RoI. For example, considering that the node radius is equal to 9 metres and the sensing area is equal to 70*80*120 m, the number of needed fixed nodes to deploy can be equal to 661, (because (70*80*120)/(4*$\pi$*92)=660,19 $\sim=$ 661); then, the initial population should be equal to 661 chromosomes randomly disseminated in the coverage area. This value is calculated assuming that 661 sensor nodes can ensure the coverage of the entire RoI in the case of a uniform deterministic deployment in the 1-coverage case (each target must be monitored by one node at least). In the case of $k$-coverage, the initial population to start with should be equal to 661 * k chromosomes.

The choice of the binary coding is justified by its easiness of use and its low computational cost (a low complexity) which is required when resolving MaOPs. Another reason is related to the use of the neighbourhood in recombination and mutation (as explained in the next section): Indeed, compared with other coding methods (such as the real coding), binary coding allows better assessing the differences in genes between two chromosomes, thus better comparing chromosomes according to their distances from each other. Nevertheless, the binary coding may lead to non-feasible solutions. These solutions will be penalized by a weighting coefficient and will not be selected by the algorithm afterwards.

Next, the used EMOs are detailed. So are the modifications proposed to enhance these algorithms in order to allow them properly handling MaOPs.

### 4.2 Including Diversity: Neighbourhood Restriction and Adaptive Multi-Operators

In MaOEAs, due to the high-dimensional objective space, the population diversity increases and mutation/crossover operators become inefficient and may create an offspring which may be not selected as a parent. To overcome this problem, the suggested mechanism relies on two strategies: an adaptive multi-recombination (multi-mutation, respectively) operators with neighbourhood restrictions, named AxN (named AmN, respectively).

#### 4.2.1 Principles of Mutation and Recombination with the Neighbourhood (AxN and AmN)

- *The neighbourhood restriction concept*

As example of the utility of using the neighbourhood in the operator's variation in MaOEAs, it is shown in [27] that MaOEAs can often apply effectively recombination to solutions having relatively similar gene structure where there is a high dependency between objectives. Thus, the neighbourhood is used aiming at improving the effectiveness of the mutation/recombination operators by increasing the number

of objectives. This helps to reduce dissimilarities between new individuals since recombining (and mutating) individuals which are too distinct may be penalizing and could affect the efficiency of the operators. To achieve this, the proposed neighbourhood concept computes the distance between individuals in the objective space. Then, it determines the set of $Nh * |P|$ nearest neighbours for each individual where |P| is the individual's population and Nh is the neighbourhood size ($Nh = |P| * 0.1$ in this study). Moreover, the proposed strategy facilitates multiple convergences by permitting higher exploitation of the move-guiding areas.

– Neighbourhood Crossover (xN)

In EMOs, the crossover operation allows generating good individuals as an offspring from parents. Ideally, this offspring must be composed of non-dominated solutions which are uniformly scattered in the population. Initially, the idea of using selection scheme mating supposes that each couple of individuals from the current population can be chosen as parents. Among the drawbacks of such mating scheme is the random choice of individuals and the large Euclidian distance between individuals in the variable space. As a consequence, the obtained solutions are more probably to be dominated. As a solution to this problem, some studies suggest a more determinist selection scheme based on the idea of considering the proximity and picking closer individuals to achieve the recombination which is very interesting for several multi-objective and many-objective problems. Thus, we propose a neighbourhood crossover that selects individuals having short Euclidian distance in the objective space so that the search ability can be reinforced by crossed individuals that are close to each other in the objective space. When crossing adjacent individuals in the variable space, the obtained offspring is generated near parent individuals in terms of their objective values and may be a non-dominated solution, which greatly increase the population diversity although the Euclidian distance in the variable space may not be defined in several cases like combinational functions. In the case of continuous functions, adjacent individuals in the objective space have often a high probability to be adjacent in the variable space. Thus, in this study, crossover is performed on adjacent individuals in the objective space instead of the variable space.

– Neighbourhood mutation (mN)

Same as the neighbourhood crossover, the neighbourhood mutation aims at restricting the production of solutions within the same niche (local area) as their parents which imply inducing a stable niching behaviour. In this study, we aim to minimize $\phi(i,j) \forall i \in V, j \in V$ where i and j are two candidate sensors to cross and $\phi$ is the distance (in the search space) between the two sensors. To perform the neighbourhood mutation, only one parameter is needed, which is the neighbourhood size ns. This parameter specifies the number of members to be considered as mutation vectors in each subpopulation. In this context, the authors in [28] investigated the effect of varying neighbourhood size on the behaviour of the algorithm. Their works prove that the preferred range of the neighbourhood size is between: 1/20 and 1/5 of the overall population. For this reason, the neighbourhood size is considered as a special niching parameter which is easy to choose since it may be taken proportionally to the population size. Thus, as proven later by the experimental results (Sect. 5), the neighbourhood size does not affect the efficiency of the algorithm. This strategy guarantees evolving each individual towards its nearest optimal point. Another advantage is the performance of the algorithm which is not dependent on the variation of the neighbourhood size.

- *The adaptive multi-operators concept*

There is another problem confronted when MOEAs are used to resolve many-objective real-world problems. This problem is the choice of the appropriate recombination and mutation operators for each problem. In the proposed strategy, the operator variations are applied adaptively. The contribution of each operator is taken into account. Indeed, the operator which succeeded in the last iteration is used to adjust the selection probability of this operator. Hence, each operator has a selection probability in the next generation which is relative to its contribution. In the adaptive mutation, the mutation probability is modified, while the algorithm is executed. This adaptive mutation relies on the feedback information from the previous generation without modifying the probabilistic nature of the mutation. Thus, new solutions are deterministically generated in the search space and are guided towards the optimum by earlier individuals.

The proposed AxN strategy is based on a crossover with neighbourhood operation which can be performed on a pair of parents after the selection step in the EMO algorithm. Indeed, we propose to use an adaptive multi-operator recombination operator which allows the improvement of the search and adapt it to the local characteristics of the problem. The AmN strategy is based on a mutation with neighbourhood operation which is used to avoid the local optima and to increase the diversity by changing the chromosomes values. The used mutation operators are chosen adaptively.

#### 4.2.2 Implementation of the AxN and AmN Strategies on the Proposed Algorithms

- $\in$-NSGA-II-AxN-AmN

Our proposed adaptive neighbour scheme of the selection operators of the $\in$-NSGA-II stems from the selection process of the AMALGAM algorithm [29], which uses a set of

MOEAs controlled by a master algorithm. The AMALGAM algorithm measures each method contribution in the previous iteration. Then, these methods are admitted according to their contributions rates exhibiting the most relevant reproductive success.

- *U-NSGA-III-AxN-AmN*

The third proposed algorithm is the U-NSGA-II-AxN-AmN which is also based on the original U-NSGA-III algorithm [25] within a modified neighbourhood mutation and recombination phase which uses adaptively all the previously indicated mutation operators.

- *MOEA/DD-AxN-AmN*

Although the original MOEA/DD [26] relies on a neighbourhood strategy, as in the previous presented algorithms, the same variations of operators are applied to the original MOEA/DD in order to take advantage of the suggested adaptive multi-operators concept.

### 4.3 Including Single-Grid and Multiple Scalarizing Functions in MOEA/DD

Among the advantages of the algorithms based on scalarizing functions compared to the algorithms based on Pareto dominance, their low-cost computation and scalability, different scalarizing functions exist. Choosing the appropriate scalarizing function is a relevant issue to be considered when designing scalarizing function-based algorithms since choosing the suitable scalarizing function is problem-dependent [30]. For example, according to [31], the weighted sum is generally used when the PF is convex, but it is not suitable for non-convex PFs. The weighted Tchebycheff is often used when the PF is non-convex, but its efficiency could be affected by the increase in the objectives number. Hence, it is interesting, to adapt the MOEA/DD, in order to have the ability to automatically choose between several scalarizing functions for each individual in each generation. Authors in [30] used two ideas for simultaneously using multiple scalarizing functions in a single MOEA/DD algorithm. The first idea is the use of several scalarizing functions in a multi-grid scheme where each scalarizing function has its unique weight vectors complete grid. The second idea is alternately assigning a different scalarizing function to every weight vector in a single grid. Their results showed that, for 0/1 knapsack problems with six objectives, simultaneously using the weighted Tchebycheff and the weighted sum in MOEA/D outperforms their individual use. However, the number of used scalarizing functions is limited to two. The aim is to use this second idea with more than two scalarizing functions. Indeed, as opposed to the original MOEA/D having a single complete grid with up to 15 weight vectors, the single-grid scheme proposed in this study relies on multiple scalarizing functions and suppose that each weight vector has a different scalarizing function. The following scalarizing functions are considered: the weighted sum (WS) [31], the weighted Tchebycheff distance (TCB) [31], the penalty-based boundary intersection (PBI) [32]. Other scalarizing functions may be considered such as the inverted PBI scalarizing function (iPBI) [32] and the vector angle distance (VA) [33]. The proposed algorithm using multiple scalarizing functions is named mMOEA/DD-AxN-AmN.

### 4.4 Including Reduction: Incorporating the Feature Selection

Since the 3D indoor deployment problem has dependent objectives, we propose to incorporate a reduction algorithm that identifies the non-essential (redundant) objectives in order to reduce the objectives number of the problem. For this purpose, an unsupervised feature selection approach is used based on the original algorithm of Mitra et al. [34]. Indeed, the feature selection is a procedure which chooses a minimum subset of correlated essential features from a given data sets in order to construct an optimal learning model to reduce the feature space dimensionality. In our context, a feature is an objective.

## 5 Experimental Results

In this section, we present the results of the proposed contributions which are experimented on a real-world problem by deploying real testbeds. The experiments are based on Arduino software programming platform and Teensyduino nodes. The proposed algorithms are implemented using the jMetal platform on an Intel core i3-3217U CPU 1.80 GHz computer. The number of constraints is determined based on the formulation proposed in Sect. 3. Unless indicated afterwards, other parameters are set as follows: the length of the area $(x) = 23.21$ m.

- Width of the area $(y) = 13.95$ m.
- Height of the area $(z) = 6.75$ m.
- Maximum execution time = 4280 s.

### 5.1 Network Architecture

The proposed network is composed of 11 fixed nodes initially deployed, 3 nomad nodes (named ‘D’, ‘E’ and ‘F’) and a mobile node (named ‘C’). The node ‘C’ is attached to a person who can move on the building. The nomad nodes to be added can be placed everywhere in the 3D space except the position where there is a fixed node or an obstacle such as a wall (several infeasible positions are discarded from the beginning by the implemented algorithms). The RSSI value of each

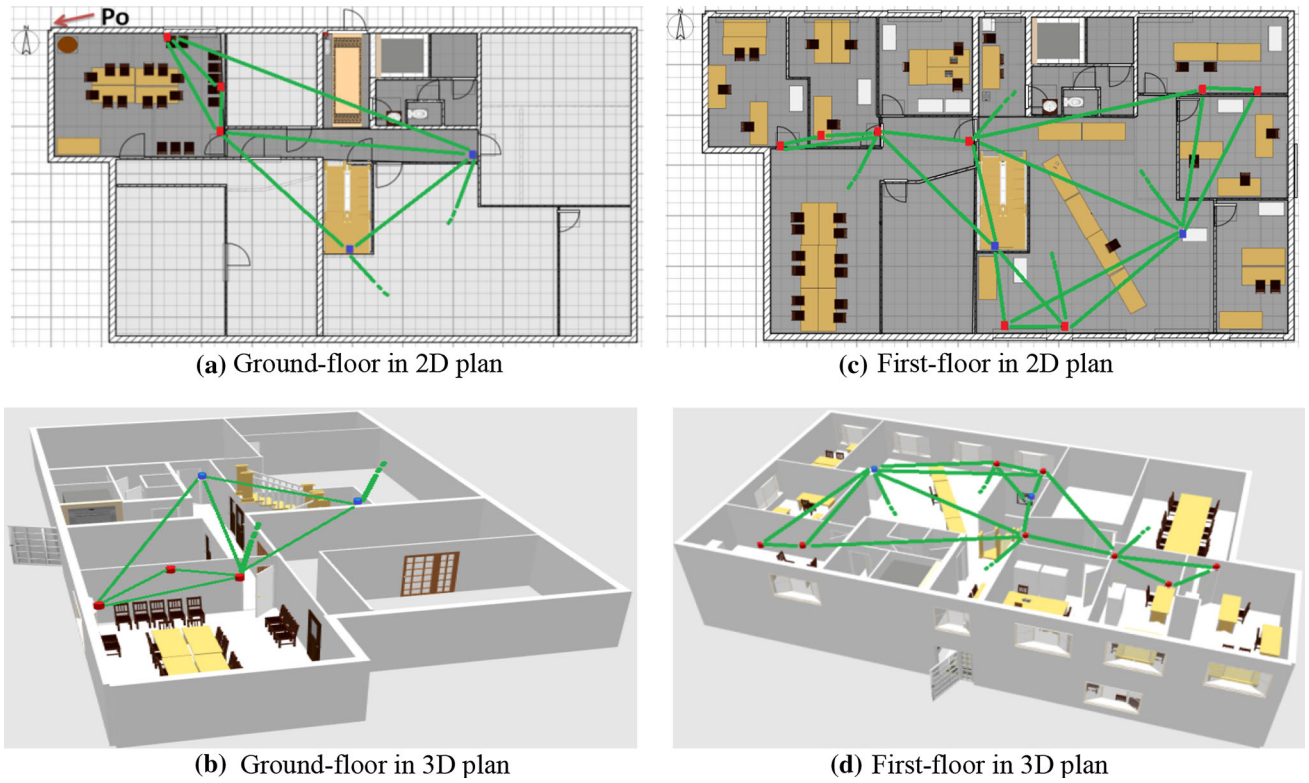


**Fig. 1** The 2D and 3D architecture of the real deployed indoor network

node is indicated by a value between 0 and 255 as shown in Figs. 2 and 3. This value can be convertible in dBm). Although the number of all deployed nodes does not exceed twenty in the experiments, the use of meta-heuristics as a resolution approach is justified, since, according to [2], the 3D deployment problem is considered as an NP-hard problem starting from two nodes to deploy. Figure 1 illustrates the deployment scheme in 2D and 3D plans. The origin of the local-taken coordinate system is set at the point $P_o$ (0,0,0) indicated in Fig. 1a. In the same figure, the nodes represented by triangles are the fixed nodes and the ones represented by circles are the nomad added nodes. The positions of the fixed nodes are chosen by the users according to their needed applicative objectives which explain the use of two nodes in the same room, while there are no ones in other rooms. The proposed deployment is considered as 3D (not a 2D multistage deployment) because of the connections between nodes situated in different floors of the building. Besides, the height of the deployed nodes is not negligible compared to the length and width of the RoI. Consequently, it is recommended to consider the indoor area as a continuous 3D space.

The technical and localization specifications of the installed nodes are listed in Table 3. Table 4 illustrates a set of chosen positions taken by the mobile node 'C' on the 3D space to assess coverage and localization. These positions are dispersed uniformly in different regions of the 3D space. In both mentioned tables, the *x* axis represents the horizontal axis, the y axis is the vertical axis, and the z axis represents the height. The point $P_o$ (0,0,0) corresponds to the following WGS84 GPS coordinates expressed in sexagesimal degrees (in degrees, minutes and seconds): latitude = 43°38′57.4″E; longitude = 1°22′28.4″E and altitude = 164 m. These GPS coordinates can be easily converted into the local coordinates using appropriate formulas.

## 5.2 Objectives

The purpose is to add nomad nodes to the indicated locations guaranteeing a set of objectives. These objectives can be either *network objectives* or *applicative objectives*. The applicative objectives represent metrics measuring physical parameters linked to sensors such as brightness, temperature or opening and closing doors. The network objectives are considered when the algorithms search the positions of the nomad nodes to add. In experiments, the considered objectives concern essentially in maximization: the *lifetime of the network*, the *coverage quality* and the *localization quality*, and in minimization: the *consumed energy* and the *hardware deployment cost*. To assess those objectives, the measurement of the links strength between nodes over time is used.

**Table 3** Localization and technical specifications of the installed node

| N° | Decimal nomenclature | Short address (the node's 16-bit address) | Type | Local-coordinate position | | |
|---|---|---|---|---|---|---|
| | | | | *X* | *Y* | *Z* |
| N1 | 01 | 0x0001 | Teensy 3.0 mk20dx128 | 278 | 545 | 523 |
| N2 | 02 | 0x0002 | Teensy 3.0 mk20dx128 | 1063 | 525 | 521 |
| N3 | 03 | 0x0003 | Teensy 3.0 mk20dx128 | 683 | 498 | 526 |
| N4 | 14 | 0x0004 | Teensy 3.1 mk20dx256 | 663 | 414 | 206 |
| N5 | 05 | 0x0005 | Teensy 3.0 mk20dx128 | 2093 | 305 | 519 |
| N6 | 06 | 0x0006 | Teensy 3.0 mk20dx128 | 1237 | 1256 | 443 |
| N7 | 15 | 0x0007 | Teensy 3.1 mk20dx256 | 450 | 00 | 290 |
| N8 | 1c* | 0x0008 | Teensy 3.1 mk20dx256 | 1114 | 1252 | 422 |
| N9 | 31* | 0x0009 | Teensy 3.1 mk20dx256 | 416 | 495 | 336 |
| N10 | 1F* | 0x000A | Teensy 3.1 mk20dx256 | 1813 | 306 | 356 |
| N11 | 34* | 0x000B | Teensy 3.1 mk20dx256 | 672 | 270 | 291 |
| N12 | 58 | 0x000D | Teensy 3.1 mk20dx256 | Variable | | |
| N13 | 59 | 0x000E | Teensy 3.1 mk20dx256 | Variable | | |
| N14 | 60 | 0x000F | Teensy 3.1 mk20dx256 | Variable | | |
| N15 | C | 0x000C | Teensy 3.1 mk20dx256 | Mobile | | |

**Table 4** Locations of the positions taken by the mobile node

| N° | | P1 | P2 | P3 | P4 | P5 | P6 | P7 | P8 | P9 | P10 | P11 | *P*12 | P13 | P14 | P15 | P16 | P17 |
|---|---|---|---|---|---|---|---|---|---|---|---|---|---|---|---|---|---|---|
| Positions on the local reference | *X* | 943 | 938 | 624 | 345 | 1152 | 1393 | 1814 | 1646 | 2148 | 1904 | 1748 | 1167 | 1693 | 865 | 362 | 1142 | 2321 |
| | *Y* | 265 | 422 | 870 | 1175 | 992 | 1197 | 1072 | 435 | 985 | 648 | 25 | 858 | 584 | 520 | 342 | 0 | 0 |
| | *Z* | 392 | 386 | 343 | 518 | 478 | 462 | 394 | 502 | 413 | 517 | 383 | 187 | 10 | 100 | 28 | 140 | 165 |

The quality of links (thus the radio coverage quality) is evaluated by measuring the FER (frame error rate). The localization quality is evaluated by measuring the RSSI, and the number of neighbours is evaluated by measuring the both mentioned metrics. The following concept is used to define a neighbour: A node 'b' is considered as a neighbour in the neighbours table of another node 'a' only if the RSSI signal of 'b', received by 'a' is sufficient (greater than a predefined tuneable threshold). We define also a predefined tuneable empirical threshold for the FER, below which a node is not considered as a neighbour. Thus, a neighbour enters in the table of neighbours only if the two mentioned thresholds are respected. Indeed, to ensure the 3D coverage, each node must have at least one neighbour and should be monitored by at least one node. As regards the localization, it is based on a hybrid 3D localization model based on 3D DV-Hop (distance vector-hop) and RSSI protocol which requires that each node must have four neighbours. Measures are taken during day and night. Indeed, the existence of persons during day implies that the majority of the doors are opened which improve the quality of the received signals. While overnight, the majority of the doors are closed.

### 5.3 Variation of the Localization

To measure the localization, a localization model based on RSSI and 3D DV-Hop hybridization is used. Indeed, the localization quality is proportional to the RSSI value. A neighbour may be included in the table of neighbours of a node only if its received RSSI value is greater than the predefined threshold (set to 100). Based on the obtained numerical results, the effect of the value of the RSSI threshold and its relationship with the FER is investigated. The value of the RSSI can change over time, and the period of its stability can be less than 1 s. Given this instability, we take an average value of RSSI extracted from four values for each pair of nodes (node i–node C); $i \in [1, 14]$. A period of waiting of 20 s between the four values is used. The RSSI value (noted $R_{ci}$) that represents the relationship between the node 'C' (the mobile node) and each node 'i' is taken as the maximum value between the detection value of 'C' by 'i' (signal generated by 'C') and the detection value of 'i' by 'C' (signal detected by 'C'). The average of the $R_{ci}$ values between 'C' and all other nodes reaching the fixed threshold in each position $P_i$ is represented by the ordinate axis in Fig. 2, expressed in the negative value of the dBm (the RSSI values between 0

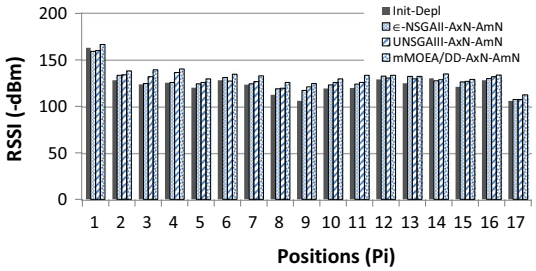


**Fig. 2** Variations of the RSSI, during day, for different positions

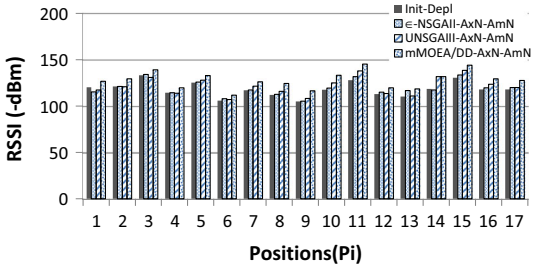


**Fig. 3** Variations of the RSSI, overnight, for different positions

and 255 are converted into values expressed in dBm), according to the proposed algorithms, by day. The horizontal axis in Fig. 2 represents the $P_i$ positions indicated in Table 4. Figure 3 shows the variation of the same RSSI averages overnight. Table I (in Appendix, ESM) illustrates the average values, in different positions $P_i$, of the RSSI classified by neighbours of the node 'C', during day. Table II (in Appendix, ESM) illustrates the average values, in different positions $P_i$, of the RSSI classified by neighbours of the node 'C', overnight. All average values in the experiments are computed based on 25 executions of the algorithms.

## 5.4 Variation of the Coverage

The FER is used as a metric to measure the coverage and to evaluate the quality of links between nodes. The above-mentioned threshold of FER (used to introduce neighbours) is fixed to 0,4. Although the FER values vary less than those of the RSSI, we take an average value of FER extracted from four values for each pair of nodes (node i–node C); $i \in [1,14]$. A period of waiting of 10 s between the four values is used. The FER value (noted $Cov_{ci}$) that represents the relationship between the mobile node 'C' and each node 'i' is considered as the average value between the detection value of 'C' by 'i' (signal generated by 'C') and the detection value of 'i' by 'C' (signal detected by 'C'). The average of the $Cov_{ci}$ values between 'C' and all other nodes reaching the fixed threshold in each position Pi is represented by the ordinate axis in Fig. 4, using the proposed algorithms, by day. The horizontal axis in Fig. 4 represents the Pi positions indicated in Table 4. Figure 5 shows the variation of the same FER averages overnight.

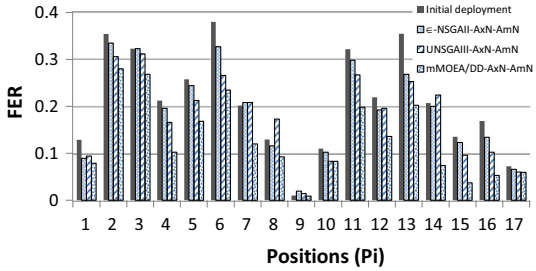


**Fig. 4** Variations of the FER, during day, in different positions

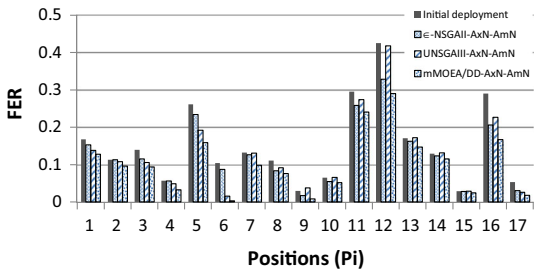


**Fig. 5** Variations of the FER, overnight, in different positions

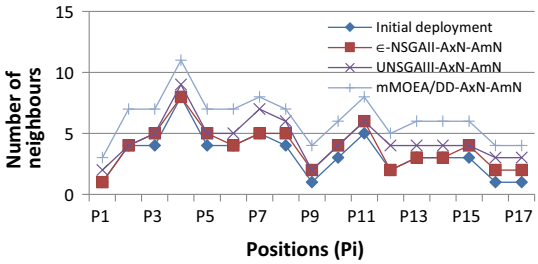


**Fig. 6** Variation of the number of neighbours, during day

Table III (in Appendix, ESM) illustrates the average values, in different positions $P_i$, of the FER, classified by neighbours of the node 'C', during day. Table IV (in Appendix, ESM) illustrates the average values, in different positions $P_i$, of the FER, classified by neighbours of the node 'C', overnight.

## 5.5 Variation of the Number of Neighbours

Figure 6 illustrates the variation on the number of neighbours, using the proposed algorithms, during day, for the $P_i$ positions. Figure 7 illustrates the variation on the number of neighbours overnight, for the same $P_i$ positions.

## 5.6 Comparing Experiments and Simulations

Using the same network architecture and parameters as in the experiments, a simulation scenario is performed using OMNeTpp. In order to compare experiments to simulations, the average number of neighbours is compared in both cases when varying the number of objectives. Figures 8, 9 and 10

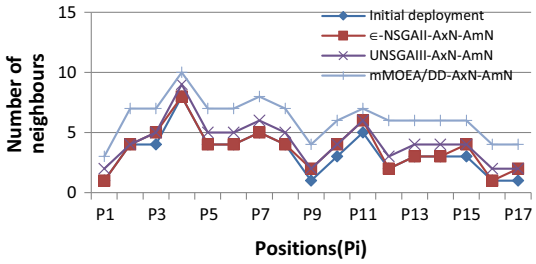


**Fig. 7** Variation of the number of neighbours, overnight

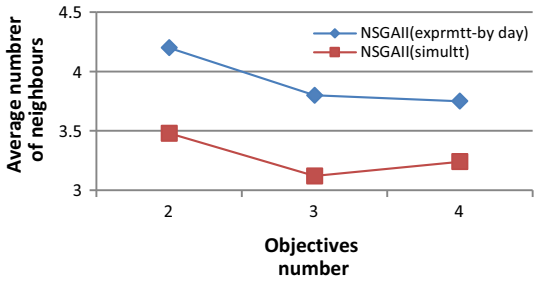


**Fig. 8** Average number of neighbours for different numbers of objectives using ∈-NSGA-II-AxN-AmN

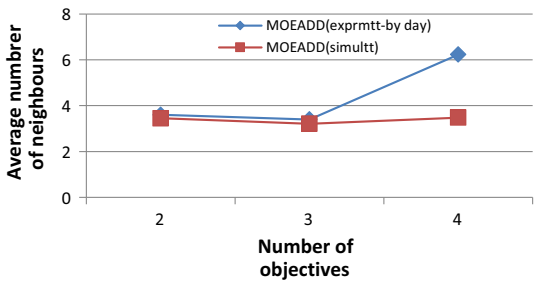


**Fig. 9** Average number of neighbours for different numbers of objectives using mMOEA/DD-AxN-AmN

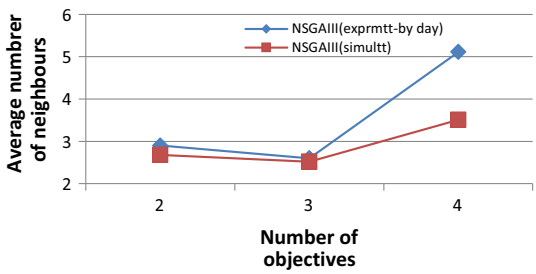


**Fig. 10** Number of neighbours for different numbers of objectives using U-NSGA-III-AxN-AmN

illustrating these comparisons show a similar behaviour, for each tested algorithm in both environments (experiments and simulations). These similarities prove the effectiveness of the proposed approach in different contexts.

### 5.7 Discussion

After the analysis of the experimental results, several findings can be considered:

- In the majority of the instances, the average of RSSI signal strength is greater during day than night because of the open doors by day, while the average of FER signal strength is greater at night than day due to less human activities at night involving less perturbations and signal interference.
- When comparing the variation of the FER and the RSSI rates between day and night, it is noted that the FER rate is higher by day than night although the RSSI rate is also higher by day than night: This indicates that the introduction of neighbours according to the highest RSSI does not always give the lowest error rate.
- The node range is not spherical: According to measures, some nodes can be detected by a set of nodes, while some other further near nodes cannot detect them. For instance, the node 'N4' is the only one that detect the node 'C' which is in the location P1 although there are other nodes which are less distant from the location P1. This assumption has been considered when implementing the proposed algorithms.
- The nature of the relationship between the RSSI and the FER is investigated: Each neighbour is introduced in the neighbours table based on a high RSSI rate, but after a moment, the rate of lost frames may be very high. Thus, increasing the RSSI value may not decrease the FER value. So, the FER indicates the quality of links better than the RSSI.
- The U-NSGA-III-AxN-AmN is more efficient in resolving the 3D deployment problem than the ∈-NSGA-II-AxN-AmN. This is due to the selection procedure of the U-NSGA-III-AxN-AmN which is based on reference points and niching. This allows more diversity among the members of the population. Although this selection procedure used on the U-NSGA-III-AxN-AmN, the ∈-NSGA-II-AxN-AmN seems to be (in several positions) more efficient than the U-NSGA-III-AxN-AmN: This occurs because the U-NSGA-III-AxN-AmN is dedicated to resolve MaOPs and may have some difficulties when objectives are high correlated (when the problem to resolve can be reduced to a bi-objective or multi-objective problem).

## 6 Numerical Results of EMOs Evaluation and Interpretations

In this section, the performance indicators and the parameters setting are presented. Afterwards, the performance of the

tested algorithms is demonstrated on the proposed real-world MaOPs: the 3D deployment in indoor WSNs optimization problem with eight objectives. This problem has seven decision variables as input and eight objectives as output. The HV is used here as an evaluation metric because of the unknown PF of the tested real-world problem. To overcome the problem of the complexity of computing the HV in our context, we compute the HV using a procedure that achieves a balance between the precision of the fitness and the cost of computation (time), so the HV computation will be possible in the many-objective case. This procedure approximates the HV based on a Monte Carlo sampling method proposed in [35].

### 6.1 Parameters Setting

The setting of the parameters affects considerably the performance of the tested algorithm when resolving a particular problem. Yet, a set of experimental tests using different sizes of population, number of objectives, number of generations and operators, are necessary when testing each MaOEA. In all tables, the best performance for each instance is shown with a *grey background*. Unless modification for testing the impact of varying the concerned parameter, the common used values of these parameters are as follows:

- *The reproduction operators* The SBX (simulated binary crossover) is used, with a large distribution index. The probability of crossover is pc = 0.9 with a distribution index $\eta c = 50$. The probability of mutation is pm = 1/400 with a distribution index $\eta m = 30$.
- *The population size and the number of reference points* Different specifications of the population size and the weight vectors number are used for each test problem. The number of reference points varies between 90 and 350. The population size varies between 100 and 1400.
- *The number of runs* To obtain statistically confident results, each algorithm is performed using 25 independent runs and a different initial population for each run.
- *The objective number* varies between 2 and 8 as follows: three objectives in minimization (the number of added nomad nodes, the hardware deployment cost and the energy consumption) and five objectives in maximization (the coverage rate, the localization rate, the connectivity rate, the lifetime and the network utilization.
- *The termination condition* (The maximum number of generations) is set to 50,000 solution evaluations.
- *The used scalarizing functions* are the weighted sum, the weighted Tchebycheff and the PBI with a penalty parameter ($\theta$ = 0.01, 0.5, 1.0 and 5.0).
- *The neighbourhood size* is fixed to 1/10 of the population size (between 1/20 and 1/5 as recommended in the Sect. 4.2.1) and the probability of selecting a parent from this neighbourhood is 0.9.

### 6.2 The Effect of the Interdependence Between Objectives

In this section, the size of the population is set to 1000. The used scalarizing function (for MOEA/DD-AxN-AmN) is PBI (0.5). The mutation probability is 1/400 (bit-flip mutation, index of 30), and the recombination probability is 0.9 [simulated binary crossover (SBX), index of 50]. No neighbour mating in recombination and the objectives are correlated (For each experiment with N objectives, at least N/2 objectives are correlated). Two hundred and fifty reference points are used for the UNGSA-III algorithm. Table 5 (Table 6, respectively) illustrates the average values of HV with non-correlated (correlated, respectively) objectives. *N* is the whole number of objectives.

**Table 5** Best, average and worst values of HV using non-correlated objectives, with 25 independent runs

| Objective number | Max Gen | ∈-NSGA-II-AxN-AmN | mMOEA/DD-AxN-AmN | UNAGSA-III-AxN-AmN |
|---|---|---|---|---|
| 3 | 400 | 0.899535 | *0.988986* | 0.983658 |
| | | 0.899492 | *0.988953* | 0.981922 |
| | | 0.899446 | *0.988911* | 0.981735 |
| 4 | 800 | 0.893884 | 0.974733 | *0.974893* |
| | | 0.893858 | 0.974578 | *0.974659* |
| | | 0.893812 | *0.974523* | 0.974468 |
| 6 | 1200 | 0.891972 | *0.972783* | 0.972589 |
| | | 0.891953 | *0.972692* | 0.972448 |
| | | 0.891927 | *0.972541* | 0.971925 |
| 8 | 1500 | 0.827925 | *0.964895* | 0.964365 |
| | | 0.827890 | *0.964772* | 0.964234 |
| | | 0.827836 | *0.964431* | 0.963827 |

**Table 6** Best, average and worst values of HV using $n$ correlated objectives ($n >= N/2$), with 25 independent runs

| Objective number | Max Gen | ∈-NSGA-II-AxN-AmN | mMOEA/DD-AxN-AmN | UNAGSA-III-AxN-AmN |
|---|---|---|---|---|
| 3 | 400 | *0.994562* | 0.994233 | 0.982356 |
| | | 0.973486 | *0.993568* | 0.981533 |
| | | 0.921357 | *0.993134* | 0.980621 |
| 4 | 800 | 0.968982 | *0.983652* | 0.977925 |
| | | 0.926065 | *0.981426* | 0.977409 |
| | | 0.925130 | *0.981124* | 0.977122 |
| 6 | 1200 | 0.921475 | *0.977123* | 0.975986 |
| | | 0.921209 | *0.976581* | 0.975574 |
| | | 0.920923 | *0.976130* | 0.975244 |
| 8 | 1500 | 0.920345 | *0.971841* | 0.967251 |
| | | 0.919803 | *0.969802* | 0.966828 |
| | | 0.919269 | *0.969023* | 0.966127 |

The obtained results show that in most cases, mMOEA/DD-AxN-AmN is more efficient than the other algorithms. Moreover, the HV increases if there is a correlation between objectives, especially in the case of the ∈-NSGA-II-AxN-AmN algorithm that has higher relative advantage improvement compared to other algorithms. As a consequence, we can conclude that ∈-NSGA-II-AxN-AmN is efficient on resolving MaOPs having highly correlated objectives.

### 6.3 The Effect of Varying the Population Size

In this section, the HV values are presented for different population sizes to test the effect of the variation in the population size on the behaviour of MaOEAs. The scalarizing function used in mMOEA/DD-AxN-AmN is PBI (0.5). The probability of mutation is 1/400 (bit-flip mutation), and the probability of recombination is 0.8 [simulated binary crossover (SBX)]. No neighbour mating of parents and the objectives are correlated. The number of reference points is chosen according to the size of the population and the number of objectives. Table 7 shows average HV values when varying the population size and the number of populations.

For the majority of the used objectives number, better results were performed by mMOEA/DD-AxN-AmN than ∈-NSGA-II-AxN-AmN. Obtained results demonstrate that the increase in the size of the population does not affect the ability of search of the mMOEA/DD-AxN-AmN. However, the ∈-NSGA-II-AxN-AmN efficiency is degraded by the increase in the population size and did not work well with large population sizes. As a result, an interesting area of research is the determination of the appropriate population size according to the number of considered objectives.

### 6.4 The Effect of the Choice of the Scalarizing Functions in MOEA/DD

Although it is proved that the mMOEA/DD-AxN-AmN performs well on DTLZ and WFG test problems, this algorithm was not evaluated on a real-world problem like ours. Moreover, its performance depends on the choice of the used scalarizing function. Thus, the choice of the appropriate scalarizing function or scalarizing function set is a relevant field of research. To overcome the problem of choosing the appropriate scalarizing function, we propose to use simultaneously several scalarizing function as described in the approach (Sect. 4). In the experiments, mMOEA/DD-AxN-AmN is applied with the weighted sum, the PBI function ($\theta = 0{,}01, 0.5, 1.0, 5.0$) and the weighed Tchebycheff with $\alpha = 1, 1.01, 1.1$. The performance of each scalarizing function is evaluated by calculating the average HV value over 25 runs. The population size in mMOEA/D-AxN-AmN was specified as 1000. The mutation probability is 1/400 (bit-flip mutation), and the recombination probability is 0.8 (SBX). No neighbour mating in recombination and the objectives are either non-correlated or correlated. The mMOEA/DD-AxN-AmN algorithm is tested using the mentioned scalarizing functions and then using the multiple scalarizing functions concept discussed previously (Sect. 4.3). Table 8 shows the average HV values when varying the scalarizing functions with different correlation relations between objectives.

According to the results in Table 8, the weighted Tchebycheff is not appropriate for the deployment problem with no (or small) dependency relation between objectives, but it is suitable when objectives are correlated. Concerning the parameter $\theta$, good results were performed by the PBI function with $\theta = 0.01$, 0.5 and 1, while the PBI with $\theta = 5$ is always the worst. Another constatation is that, except for small penalty ($\theta$) values, the deterioration of the

**Table 7** Best, average and worst HV with different population sizes and objectives number

| Objective number | Population size | ∈-NSGA-II-AxN-AmN | mMOEA/DD-AxN-AmN | UNAGSA-III-AxN-AmN | Number of reference points/ weigh vectors (U-NSGA-III/ MOEA/DD ) |
|---|---|---|---|---|---|
| 4 | 100 | 0.927985 | *0.983461* | 0.976237 | 90 |
| | | 0.927109 | *0.982320* | 0.975698 | |
| | | 0.926568 | *0.982029* | 0.975205 | |
| | 500 | 0.928631 | *0.985237* | 0.976844 | 130 |
| | | 0.928028 | *0.984562* | 0.976004 | |
| | | 0.927563 | *0.984103* | 0.975236 | |
| | 1000 | 0.929870 | 0.985992 | *0.986773* | 255 |
| | | 0.928124 | *0.985128* | 0.976165 | |
| | | 0.928007 | *0.984536* | 0.975896 | |
| | 1200 | 0.928896 | 0.986213 | *0.987971* | 280 |
| | | 0.928364 | *0.985897* | 0.975884 | |
| | | 0.928103 | *0.985251* | 0.974656 | |
| | 1400 | 0.928987 | *0.986852* | 0.976852 | 290 |
| | | 0.928657 | *0.986238* | 0.975366 | |
| | | 0.927223 | *0.985140* | 0.975101 | |
| 8 | 100 | 0.915631 | *0.970145* | 0.967334 | 90 |
| | | 0.914122 | *0.969233* | 0.966785 | |
| | | 0.914033 | *0.969002* | 0.966176 | |
| | 500 | 0.919778 | *0.969986* | 0.967889 | 230 |
| | | 0.919266 | *0.969645* | 0.967034 | |
| | | 0.919025 | *0.969023* | 0.965361 | |
| | 1000 | 0.920244 | 0.970243 | *0.971913* | 320 |
| | | 0.919963 | *0.969886* | 0.967362 | |
| | | 0.919332 | *0.969122* | 0.966772 | |
| | 1200 | 0.921563 | *0.970274* | 0.968946 | 350 |
| | | 0.919255 | *0.969962* | 0.967691 | |
| | | 0.918334 | *0.969146* | 0.967123 | |
| | 1400 | 0.920477 | *0.970988* | 0.968214 | 350 |
| | | 0.919876 | *0.970231* | 0.967983 | |
| | | 0.919241 | *0.969862* | 0.967227 | |

performance of mMOEA/DD-AxN-AmN when increasing the objectives number was less clear when using the PBI than the weighted Tchebycheff function. Moreover, using high penalty values, the mMOEA/DD-AxN-AmN encountered difficulties in finding better solutions with respect to the weighted Tchebycheff function than the PBI. Besides, it is concluded from results that the weighed sum is not suitable for bi-objective problems, but it is a good choice for four to eight objectives problems. Furthermore, for most instances, the simultaneous use of scalarizing functions gives better results than individually using scalarizing functions. For further investigations, the evolution of the number of non-dominated solutions according to the size of the population, using different scalarizing functions, can be studied.

### 6.5 The Effect of Using Neighbourhood Restrictions and Adaptive Operators

In this section, the efficiency of the proposed strategies based on mating similar parents and adaptive mutation and crossover operators (AxN and AmN) is examined. The performance of each algorithm is assessed using the average HV over 25 runs. The population size in mMOEA/DD-AxN-AmN was set to 1000. The mutation probability is 1/400, and the recombination probability is 0.8. Neighbour mating is performed in recombination, and the objectives are correlated. The number of reference points is set to 100. Table 9 shows average HV values when using the neighbourhood restrictions and adaptive operators.

**Table 8** Best, average and worst values of HV with different scalarizing functions

| | Objective number | Weighted sum | Weighted Tchebycheff | PBI ($\theta = 0.01$) | PBI ($\theta = 0.5$) | PBI ($\theta = 1$) | PBI ($\theta = 5$) | Our implementation** |
|---|---|---|---|---|---|---|---|---|
| Non-correlated objectives | 2 | 0.665895 | 0.976314 | 0.954122 | 0.957326 | 0.955232 | 0.949963 | *0.979107* |
| | | 0.665210 | 0.975235 | 0.953954 | 0.953623 | 0.953488 | 0.946126 | *0.978685* |
| | | 0.664339 | 0.974566 | 0.953203 | 0.952003 | 0.950536 | 0.945224 | *0.978022* |
| | 4 | 0.854369 | 0.789992 | 0.973220 | *0.977998* | 0.974351 | 0.972783 | 0.976324 |
| | | 0.853201 | 0.789125 | 0.972674 | 0.972463 | 0.972367 | 0.971806 | *0.975788* |
| | | 0.852874 | 0.788331 | 0.972003 | 0.972026 | 0.971974 | 0.968122 | *0.975002* |
| | 6 | 0.867922 | 0.783261 | 0.971852 | 0.972633 | 0.972678 | 0.969982 | *0.975457* |
| | | 0.867364 | 0.782975 | 0.970556 | 0.972022 | 0.972135 | 0.969856 | *0.974985* |
| | | 0.866893 | 0.782023 | 0.968423 | 0.971881 | 0.971364 | 0.969634 | *0.974454* |
| | 8 | 0.869233 | 0.780968 | 0.962344 | 0.971989 | 0.972336 | 0.969877 | *0.974623* |
| | | 0.868809 | 0.780661 | 0.961913 | 0.971456 | 0.971874 | 0.969233 | *0.974161* |
| | | 0.868469 | 0.780424 | 0.961599 | 0.971123 | 0.971299 | 0.969024 | *0.974022* |
| Correlated objectives | 2 | 0.668644 | 0.982897 | *0.984442* | 0.954221 | 0.954330 | 0.948433 | 0.982889 |
| | | 0.667985 | 0.982468 | *0.983843* | 0.953965 | 0.953987 | 0.947852 | 0.982347 |
| | | 0.667362 | 0.982022 | *0.983110* | 0.953246 | 0.953224 | 0.948911 | 0.982102 |
| | 4 | 0.859212 | 0.793066 | *0.981988* | 0.973366 | 0.973784 | 0.972922 | 0.981843 |
| | | 0.858548 | 0.792653 | *0.981416* | 0.972974 | 0.973166 | 0.972349 | 0.981324 |
| | | 0.858009 | 0.792023 | *0.981124* | 0.972231 | 0.972038 | 0.972121 | 0.981006 |
| | 6 | 0.868983 | 0.783877 | 0.980986 | 0.973465 | 0.974354 | 0.970963 | *0.981877* |
| | | 0.868244 | 0.783366 | 0.980574 | 0.972896 | 0.972846 | 0.970684 | *0.981213* |
| | | 0.868013 | 0.782783 | 0.980129 | 0.972234 | 0.972023 | 0.970261 | *0.980688* |
| | 8 | 0.869867 | 0.781782 | *0.981235* | 0.972356 | 0.972852 | 0.970979 | 0.973982 |
| | | 0.869136 | 0.781144 | *0.979815* | 0.971964 | 0.972133 | 0.970318 | 0.973564 |
| | | 0.868874 | 0.780633 | 0.978248 | 0.971211 | 0.971646 | 0.970002 | *0.978421* |

**Based on single-grid and simultaneously used multiple scalarizing functions

**Table 9** Best, average and worst HV with neighbourhood restrictions and adaptive operators

| | Objective number | ∈-NSGA-II-AxN-AmN | mMOEA/DD-AxN-AmN | UNAGSA-III-AxN-AmN |
|---|---|---|---|---|
| Bit-flip mutation/SBX crossover | 4 | 0.928687 | *0.983475* | 0.979325 |
| | | 0.926324 | *0.981874* | 0.977693 |
| | | 0.925714 | *0.979371* | 0.977102 |
| | 8 | 0.919879 | *0.970251* | 0.967351 |
| | | 0.919235 | *0.969682* | 0.966487 |
| | | 0.918953 | *0.968337* | 0.966022 |
| Using AxN and AmN | 4 | 0.944941 | *0.983129* | 0.980369 |
| | | 0.940239 | *0.981952* | 0.979121 |
| | | 0.929782 | *0.980237* | 0.978922 |
| | 8 | 0.920174 | 0.971002 | *0.971352* |
| | | 0.919877 | *0.970254* | 0.966964 |
| | | 0.919003 | *0.968968* | 0.962237 |

**Table 10** Comparing according to the best, average and worst HV values

| Original objective number | Reduced objective number | HV using the feature selection (applied on the reduced objective set) | | |
|---|---|---|---|---|
| | | ∈-NSGA-II-AxN-AmN | mMOEA/DD-AxN-AmN | UNAGSA-III-AxN-AmN |
| 4,5 | 3 | 0.899535 | *0.988986* | 0.983658 |
| | | 0.899492 | *0.988953* | 0.981922 |
| | | 0.899446 | *0.988911* | 0.981735 |
| 6 | 4 | 0.893884 | 0.974733 | *0.974893* |
| | | 0.893858 | 0.974578 | *0.974659* |
| | | 0.893812 | *0.974523* | 0.974468 |
| 8 | 6 | 0.891972 | *0.972783* | 0.972589 |
| | | 0.891953 | *0.972692* | 0.972448 |
| | | 0.891927 | *0.972541* | 0.971925 |

Obtained results with different numbers of objectives indicate that AxN and AmN improve considerably the search performance. Better results were obtained for different numbers of objectives on the mMOEA/DD-AxN-AmN algorithm. When the number of objectives increases, the efficiency of mMOEA/DD-AxN-AmN over ∈-NSGA-II-AxN-AmN becomes clearer. Despite this, much larger improvement in the average HV value (with and without similar parent recombination) was obtained by ∈-NSGA-II-AxN-AmN than other algorithms. Moreover, results prove that mating similar parents improves the diversity without deteriorating the convergence.

### 6.6 The Effect of Incorporating the Reduction Based on Feature Selection

In order to test the effect of reducing the objectives using the feature selection, we measure the HV (the best, average and worst values) issued from the proposed evolutionary algorithm, when incorporating the feature selection procedure. Objectives are correlated. Table 10 illustrates the results.

## 7 Conclusions and Perspectives

This paper aims to propose a deployment scheme in 3D indoor wireless sensor networks. Different objectives are considered. Three modified variants of the ∈-NSGA-II, the U-NSGA-III and the MOEA/DD algorithms are proposed. Different mutation operators are involved using and adaptive neighbourhood method of operator's selection. Moreover, we investigate the proposed algorithms on a real deployed testbed with real assumptions in the 3D case. The results prove that the aggregation-based approach (MOEA/DD) is generally more efficient than the other proposed algorithms in resolving the 3D indoor deployment problem. In addition, it is proven that the adaptive method of selection of mutation and recombination operators with neighbourhood restrictions improves the efficiency of the algorithms. Besides, we

assess the behaviour of the algorithms when incorporating a feature selection dimensionality reduction procedure. In the future, different directions can be investigated. We can further use a large-scale grid of nodes (as the IOT-Lab [36]) to test the scalability and the behaviour of the proposed algorithms in large scale. Moreover, we are working on well-studied and justified hybridizations of EMOs by incorporating the user preferences to minimize the execution time and the complexity of the studied MaOP.

## References


1. Saipulla, A.; Cui, J.; Fu, X.; Liu, B.; Wang J.: Barrier coverage: foundations and design. In: The Art of Wireless Sensor Networks, Volume 2: Advanced Topics and Applications, 1st ed., pp. 59–115. Springer, Berlin. eBook ISBN 978-3-642-40066-7. Hardcover ISBN 978-3-642-40065-0. Series ISSN 1860-4862 (2014). https://doi.org/10.1007/978-3-642-40066-7
2. Cheng, X.; Du, D.Z.; Wang, L.; Xu, B.: Relay sensor placement in wireless sensor networks. ACM/Springer J. Wirel. Netw. **14**(3), 347–355 (2008). https://doi.org/10.1007/s11276-006-0724-8
3. Mansoor, U.; Ammari, H. M.: Coverage and connectivity in 3D wireless sensor networks. In: The Art of Wireless Sensor Networks, Volume 2: Advanced Topics and Applications, 1st ed., Springer, Berlin, pp. 273–324 (2014). https://doi.org/10.1007/978-3-642-40066-7
4. Shah, B.; Kim, K.: A survey on three-dimensional wireless ad hoc and sensor networks. Int. J. Distrib. Sens. Netw. **10**(7), 616014 (2014). https://doi.org/10.1155/2014/616014
5. Jiang, J.A.; Wan, J.J.; Zheng, X.Y.; Chen, C.P.; Lee, C.H.; Su, L.K.; Huang, W.C.: A novel weather information-based optimization algorithm for thermal sensor placement in smart grid. IEEE Trans. Smart Grid **PP**(99), 1–11 (2016). https://doi.org/10.1109/TSG.2016.2571220
6. Alia, O.M.; Al-Ajouri, A.: Maximizing wireless sensor network coverage with minimum cost using harmony search algorithm. IEEE Sens. J. **17**(3), 882–896 (2017). https://doi.org/10.1109/JSEN.2016.2633409
7. Sweidan, H.I.; Havens, T. C.: Coverage optimization in a terrain-aware wireless sensor network. In: Proceedings of the 2016 IEEE Congress on Evolutionary Computation (CEC), Vancouver, BC, pp. 3687–3694 (2016). https://doi.org/10.1109/CEC.2016.7744256
8. Khalfallah, Z.; Fajjari, N.; Aitsaadi, Rubin P.; Pujolle, G.: A novel 3D underwater WSN deployment strategy for full-coverage and connectivity in rivers. In: IEEE International Conference on Communications (ICC), Kuala Lumpur, 2016, pp. 1–7. https://doi.org/10.1109/ICC.2016.7510979
9. Brown, T.; Wang, Z.; Shan, T.; Wang, F.; Xue, J.: On wireless video sensor network deployment for 3D indoor space coverage, SoutheastCon, Norfolk, VA, 2016, pp. 1–8. https://doi.org/10.1109/SECON.2016.7506744
10. Liu, Z.; Ouyang, Z.: k-Coverage estimation problem in heterogeneous camera sensor networks with boundary deployment. IEEE Access **6**, 2825–2833 (2018). https://doi.org/10.1109/ACCESS.2017.2785393
11. Cotta, C.; Gallardo, J.E.: Metaheuristic approaches to the placement of suicide bomber detectors. J. Heuristics **24**(3), 483–513 (2018). https://doi.org/10.1007/s10732-017-9335-z
12. Wu, C.Q.; Wang, L.: On efficient deployment of wireless sensors for coverage and connectivity in constrained 3D space. Sensors (Basel) **17**(10), 2304 (2017). https://doi.org/10.3390/s17102304
13. Hu, J.; Luo, J.; Zheng, Y.; Li, K.: Graphene-grid deployment in energy harvesting cooperative wireless sensor networks for green IoT. IEEE Trans. Ind. Inform. (2018)
14. Zhang, S; Jiajia, L.: Analysis and Optimization of Multiple Unmanned Aerial Vehicle-Assisted Communications in Post-Disaster Areas. IEEE Transactions on Vehicular Technology. pp(99):1-1, (2019). https://doi.org/10.1109/TVT.2018.2871614
15. Zhang, S.; Jiajia, L.: Analysis and optimization of multiple unmanned aerial vehicle-assisted communications in post-disaster areas. IEEE Trans. Veh. Technol. **99**, 1–1 (2019). https://doi.org/10.1109/TVT.2018.2871614
16. Cao, B.; Zhao, J.; Yang, P.; Ge Lv, Z.; Liu, X.; Min, G.: 3D multi-objective deployment of an industrial wireless sensor network for maritime applications utilizing a distributed parallel algorithm. IEEE Trans. Ind. Inform. (2018). https://doi.org/10.1109/TII.2018.2803758
17. Cui, W.; Zeng, L.; Li, Q.; Zhang, Y.; Liang, J.: Deployment of 3D wireless sensors within forest based on genetic algorithm. In: Liang, Q.; Mu, J.; Jia, M.; Wang, W.; Feng, X.; Zhang, B. (eds.) Communications, Signal Processing, and Systems. CSPS. Lecture Notes in Electrical Engineering, vol. 463 (2019) Springer, Singapore
18. Zhou, Y.; Wang, H.; Li, S.: Research on the deployment algorithm of distributed detection network. In: Liang, Q.; Mu, J.; Jia, M.; Wang, W.; Feng, X.; Zhang, B. (eds.) Communications, Signal Processing, and Systems. CSPS 2017. Lecture Notes in Electrical Engineering, vol. 463. (2019). Springer, Singapore
19. Hildmann, H.; Atia, D.Y.; Ruta, D.; Poon, K.; Isakovic, A. F.: Nature-Inspired optimization in the era of IoT: particle swarm optimization (PSO) applied to indoor distributed antenna systems (I-DAS). In: Elfadel, I.; Ismail, M. (eds.) The IoT physical layer. Springer, Cham (2019) (forthcoming). https://doi.org/10.1007/978-3-319-93100-5_11
20. Asorey-Cacheda, R.; Garcia-Sanchez, A.-J.; Garcia-Sanchez, F.; Garcia-Haro, J.: A survey on non-linear optimization problems in wireless sensor networks. J. Netw. Comput. Appl. **82**, 1–20 (2017). https://doi.org/10.1016/j.jnca.2017.01.001
21. Das, S.; Debbarma, M.K.: A survey on coverage problems in wireless sensor network based on monitored region. In: Kolhe, M.; Trivedi, M.; Tiwari, S.; Singh, V. (eds.) Advances in Data and Information Sciences. Lecture Notes in Networks and Systems, vol. 39. (2019). Springer, Singapore. https://doi.org/10.1007/978-981-13-0277-0_29
22. Maheshwari, A.; Chand, N.: A survey on wireless sensor networks coverage problems. In: Krishna, C.; Dutta, M.; Kumar R. (eds.) Proceedings of 2nd International Conference on Communication, Computing and Networking. Lecture Notes in Networks and Systems, vol. 46. pp 153–164 (2019). Springer, Singapore. https://doi.org/10.1007/978-981-13-1217-5_16
23. Meribout, M.; Al Naamany, A.: A collision free data link layer protocol for wireless sensor networks and its application in intelligent transportation systems. In: Wireless Telecommunications Symposium, Prague, pp. 1-6. (2009). https://doi.org/10.1109/WTS.2009.5068957
24. Kollat, J.B.; Reed, P.: Comparison of multi-objective evolutionary algorithms for long-term monitoring design. Adv. Water Resour. **29**(6), 792–807 (2006)
25. Seada, H.; Deb, K.: A unified evolutionary optimization procedure for single, multiple, and many objectives. IEEE Trans. Evol. Comput. **20**(03), 358–369 (2016). https://doi.org/10.1109/TEVC.2015.2459718
26. Li, K.; Deb, K.; Zhang, Q.; Kwong, S.: An evolutionary many-objective optimization algorithm based on dominance and decomposition. IEEE Trans. Evol. Comput. **19**(5), 694–716 (2015). https://doi.org/10.1109/TEVC.2014.2373386

27. Ishibuchi, H.; Akedo, N.; Nojima, Y.: Behavior of multi-objective evolutionary algorithms on many-objective knapsack problems. IEEE Trans. Evol. Comput. **19**(2), 264–283 (2015)
28. Qu, B.Y.; Suganthan, P.N.; Liang, J.J.: Differential evolution with neighborhood mutation for multimodal optimization. IEEE Trans. Evol. Comput **16**(5), 601–614 (2012)
29. Vrugt, J.A.; Robinson, B.A.: Improved evolutionary optimization from genetically adaptive multimethod search. Proc. Natl. Acad. Sci. U.S.A. **104**(3), 708–711 (2007). https://doi.org/10.1073/pnas.0610471104
30. Ishibuchi, H.; Sakane, Y.; Tsukamoto, N.; Nojima, Y.: simultaneous use of different scalarizing functions in MOEA/D. In: 12th Annual Conference on Genetic and Evolutionary Computation GECCO, pp. 519–526 (2010)
31. Ishibuchi, H.; Sakane, Y.; Tsukamoto, N.; Nojima, Y.: Adaptation of scalarizing functions in MOEA/D: an adaptive scalarizing function-based multiobjective evolutionary algorithm. In: Proceedings of the EMO 2009, LNCS 5467, pp. 438–452 (2009)
32. Sato., H.: Inverted PBI in MOEA/D and its impact on the search performance on multi and many-objective optimization. In: Proceedings of the 16th Annual Conference on Genetic and Evolutionary Computation (GECCO), pp. 645–652 (2014)
33. Tan, Y.; Jiao, Y.; Li, H.; Wang, X.: MOEA/D + uniform design: A new version of MOEA/D for optimization problems with many objectives. Comput. Oper. Res. **40**(6), 1648–1660 (2013)
34. Mitra, P.; Murthy, C.A.; Pal, S.K.: Unsupervised feature selection using feature similarity. IEEE Trans. Pattern Anal. Mach. Intell **24**(3), 301–312 (2002). https://doi.org/10.1109/34.990133
35. Bader, J.; Zitzler, E.: HypE: an algorithm for fast hypervolume-based many-objective optimization. Evol. Comput. **19**(1), 45–76 (2011)
36. The IOTLab platform: software available at http://www.iot-lab.info (2018). Accessed on October 08th (2018)